

Geometro-thermodynamics of tidal charged black holes

László Árpád Gergely^{1,2}, Narit Pidokrajt³, Sergei Winitzki⁴

¹ *Department of Theoretical Physics, University of Szeged,*

Tisza Lajos krt 84-86, Szeged 6720, Hungary

² *Department of Experimental Physics,*

University of Szeged, Dóm Tér 9, Szeged 6720, Hungary

³ *Department of Physics, Stockholm University, 106 91 Stockholm, Sweden*

⁴ *Arnold Sommerfeld Center for Theoretical Physics,*

Department of Physics, Ludwig-Maximilians University,

Theresienstr. 37, 80333 Munich, Germany

(Dated: November 1, 2018)

Abstract

Tidal charged spherically symmetric vacuum brane black holes are characterized by their mass m and tidal charge q , an imprint of the 5-dimensional Weyl curvature. For $q > 0$ they are formally identical to the Reissner-Nordström black hole of general relativity. We study the thermodynamics and thermodynamic geometries of tidal charged black holes and discuss similarities and differences as compared to the Reissner-Nordström black hole. As a similarity, we show that (for $q > 0$) the heat capacity of the tidal charged black hole diverges on a set of measure zero of the parameter space, nevertheless both the regularity of the Ruppeiner metric and a Poincaré stability analysis shows no phase transition at those points. The thermodynamic state spaces being different indicates that the underlying statistical models could be different. We find that the $q < 0$ parameter range, which enhances the localization of gravity on the brane, is thermodynamically preferred. Finally we constrain for the first time the possible range of the tidal charge from the thermodynamic limit on gravitational radiation efficiency at black hole mergers.

I. INTRODUCTION

Thermodynamics of black holes (BHs) was formulated almost 40 years ago by Bardeen, Carter and Hawking [1]. The Bekenstein-Hawking entropy is proportional to the area of the event horizon and it reads

$$S = \frac{c^3 k_B A}{4G\hbar} , \quad (1)$$

where c, k_B, G and \hbar are speed of light, Boltzmann's constant, Newton's gravitational constant and the reduced Planck's constant, respectively and A represents the area of the horizon.

Despite the fact that BH thermodynamics is well established, there is no controlled calculation of BH entropy based on standard statistical mechanics which associates entropy with a large number of microstates. The first paper on the BH's microstate counting appeared in 1996 by Strominger and Vafa [2] who were able to calculate the Bekenstein-Hawking entropy of a five-dimensional extremal BH in the framework of string theory. Since then there have been a growing number of papers on this topic.

An alternative way to study BH thermodynamics phenomenologically is by studying a certain pseudo-Riemannian geometry defined on the thermodynamic state space (the parameter space). A "thermodynamical" metric known as the Ruppeiner metric is defined as the negative of the Hessian of the entropy S with respect to the mass m and other extensive parameters q^i , including electric charge and angular momentum:

$$g_{ab}^R = -\partial_a \partial_b S(m, q^i) . \quad (2)$$

The first paper on the subject is by Ruppeiner [3]; a review on the application to various thermodynamic systems is given in [4]. The Ruppeiner geometry of anyon gas has also been worked out [5].

The Ruppeiner geometry is one particular type of information geometry [6]. Ruppeiner originally developed his theory in the context of thermodynamic fluctuation theory, for systems in canonical ensembles. Many BHs have *negative* specific heats and are described microcanonically. For systems with non-interacting underlying statistical models, such as the ideal gas, the Ruppeiner geometry is flat [3]. Singularities in the curvature of the Ruppeiner metric signal thermodynamic instabilities of the system in question.

The most physically significant result as reported in [7] is that the Myers-Perry Kerr BH ultra-spinning instability is hinted by the Ruppeiner geometry. More precisely, the curvature singularities

of the Ruppeiner metric signal the onset of ultraspinning instabilities of the Myers-Perry Kerr BHs in dimensions $D > 5$, found earlier by Emparan and Myers [8].

In [10] it was shown that the Ruppeiner metric for a two-dimensional thermodynamic state space is flat, provided the entropy takes the power-law form $S = m^p f(Q/m)$ for any $p \neq 1$, where Q represents a conserved charge (the angular momentum in the case of the spinning Kerr BH). This theorem is useful when one wants to quickly rule out thermodynamic curvature singularities of the system. Certain BHs do have flat Ruppeiner metric, *e.g.* Reissner-Nordström (RN), BTZ, and 4-dimensional Einstein-Maxwell-dilaton BHs. Well known examples of BHs with non-flat Ruppeiner geometry include Kerr, Kerr-Newman, and Reissner-Nordström-AdS BHs [9]. Recent papers on applications of the Ruppeiner geometry to BH thermodynamics are listed in [11]-[19]. Thermodynamic geometry has been accepted as one of the standard tools used in investigating whether instability or critical phenomena is present in a given thermodynamic system.

An alternative geometric approach to thermodynamics is given by the Weinhold metric [20], which is defined as the Hessian of the mass (internal energy) with respect to entropy and other extensive parameters such as charge, angular momentum, etc.

$$g_{ab}^W = \partial_a \partial_b m(S, q^i) . \quad (3)$$

The Weinhold metric is equal to the conformally rescaled Ruppeiner metric,

$$g^W = T g^R , \quad (4)$$

where it is understood that both metrics have been transformed to the same set of coordinates. The conformal factor T is the temperature,

$$T = \partial_S m = \frac{1}{\partial_m S} . \quad (5)$$

The relationship (4) has been derived previously using involved thermodynamical arguments [21]. We present in Appendix B a generic and simple proof of the statement (4).

Black hole solutions arise not only in general relativity and string theory, but also in brane-world gravity models. There are many brane-world scenarios, but in the simplest gravity evolves in a curved 5D space-time (the bulk), which contains a temporal 4D hypersurface (the brane), on which all the fields of the standard model are localized. Gravitational dynamics on the brane is governed by an effective Einstein equation [22]-[24].

The most well-known brane BH is the spherically symmetric vacuum *tidal* charged BH, derived in [25]:

$$ds^2 = -f(r) dt^2 + f^{-1}(r) dr^2 + r^2 (d\theta^2 + \sin^2 \theta d\varphi^2) . \quad (6)$$

The metric function f is given as

$$f(r) = 1 - \frac{2m}{r} + \frac{q}{r^2}. \quad (7)$$

Such BHs are characterized by two parameters: their mass m and tidal charge q . The latter arises from the Weyl curvature of the 5D space-time into which the brane is embedded (more exactly, from its “electric” part as computed with respect to the brane normal).

Formally the metric (6) agrees with the Reissner-Nordström solution of a spherically symmetric Einstein-Maxwell system in general relativity, provided we replace the tidal charge q by the square of the *electric* charge Q . Thus $q = Q^2$ is always positive, when the metric (6) describes the spherically symmetric exterior of an electrically charged object in general relativity. By contrast, in brane-world theories the metric (6) allows for any sign of q . A positive tidal charge weakens the gravitational field of the BH in precisely the same way the electric charge of the Reissner-Nordström BH does. A negative tidal charge, however, strengthens the gravitational field, contributing to the localization of gravity on the brane.

The structure of the tidal charged BH in the case $q > 0$ is in full analogy with the general relativistic Reissner-Nordström solution¹. For $0 < q < m^2$ it describes tidal charged BHs with two horizons, located at $r_{\pm} = m \pm \sqrt{m^2 - q}$, both below the Schwarzschild radius. For $q = m^2$ the two horizons coincide at $r_e = m$ (this is the analogue of the extremal Reissner-Nordström BH). For any $q < 0$ there is only one horizon, at $r_+ = m + \sqrt{m^2 + |q|}$. For these BHs, gravity is increased on the brane by the presence of the tidal charge. This contributes towards the localization of gravity on the brane.

Although the full 5-dimensional solution containing the tidal charged BH as the brane section remains unknown, very recently it has been proven at a perturbative level, that when the tidal charged contribution dominates over the Schwarzschild contribution, the horizon does close in the fifth dimension, therefore the tidal charged brane BH becomes a section of a 5-dimensional BH with regular horizon [27] (see also the related Ref. [28]).

Work on the tidal charged BH includes the matching with an interior stellar solution, a procedure requiring a negative q [29], the study of weak deflection of light to second order in both parameters [30], [31], the study of weak gravitational lensing by tidal charged BH [32], a confrontation with solar system tests [33], and the evolution of thin accretion disks in this geometry [34].

¹ In making analogy with the RN BH one can also consider the Born-Infeld BHs, which is a nonlinear generalization of the RN BH [26]

In this paper we analyze the tidal charged BH both by standard thermodynamic and geometric methods provided by the thermodynamic metrics. Emparan, Horowitz and Myers have constructed a lower-dimensional toy model with BTZ BHs on the brane, which are BTZ “black strings” in the bulk [35]. They were able to show that the four-dimensional entropy computed from the horizon area agrees (to a leading order at large mass) with the three-dimensional entropy computed from the circumference of the horizon. The two definitions of the entropy differed in the number of dimensions and in the value of the corresponding Planck masses. Therefore the result of [35] can be taken as a hint that there are thermodynamic constraints on the 5D extension of the tidal charged BH, which are provided by our present analysis.

In Section II we discuss the mass and tidal charge dependence of the entropy of the tidal charged BH. We compute the temperature and analyze the heat capacity at constant q . Then in Section III we study in detail the Ruppeiner and Weinhold geometries of the tidal charged BH, pointing out similarities and differences with respect to the Reissner-Nordström BH. The geodesic structure for both information geometries is presented in Appendix.

One major concern is the stability of any BH solution. This can be investigated by thermodynamics means. In this context it has been shown that for charged AdS BHs the plot of $1/T$ vs. horizon area is quite similar to the (p, V) diagram of the Van der Waals gas, indicating phase transitions [36]. Based on our analysis we will prove in Section IV that the tidal charged BHs are stable, regardless of the sign of the tidal charge. Then, in Section V we restrict for the first time the range of the tidal charge, based on thermodynamic limits on gravitational radiation efficiency at BH mergers.

Finally we discuss our results in the concluding section.

II. THERMODYNAMIC CONSIDERATIONS

A. Entropy and mass

The exterior horizon for $q > 0$ or the single horizon for $q < 0$ are both given by

$$r_+ = m + \Theta, \quad (8)$$

where we have introduced the shorthand notation $\Theta = \sqrt{m^2 - q}$, real for any $q \leq m^2$. The BH’s entropy (1) in geometrized units and $k_B = 1/\pi$ reads,

$$S = \frac{A}{4\pi} = r_+^2 = (m + \Theta)^2. \quad (9)$$

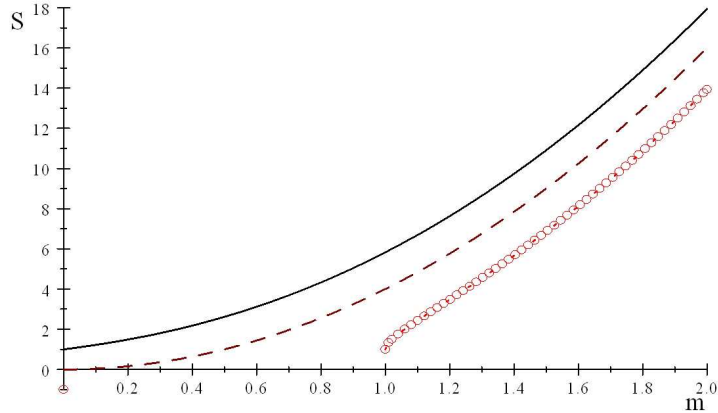


Figure 1: The entropy always increases with the mass. The plots are for negative tidal charged BH with $q = -1$ (solid line), Schwarzschild BH with $q = 0$ (dashed line) and positive charged tidal BH with $q = 1$ (dotted line). In the latter case one can see that the entropy is not defined for masses below the extremal limit $m < \sqrt{q}$.

It is instructive to see the variation of entropy with the BH parameters. The entropy increases with mass (Fig. 1). By contrast, the entropy decreases with increasing q (irrespective of the sign of q) until $S = m^2$ and the minimal horizon area $A = 4\pi m^2$ are reached at the extremal limit $q = m^2$ (Fig. 2). This is to be expected since for $q > m^2$ the metric (6) describes a naked singularity (thus the area A is undefined).

We can also express the mass of the tidal charged BH in terms of entropy and tidal charge:

$$m = \frac{\sqrt{S}}{2} \left(1 + \frac{q}{S} \right). \quad (10)$$

The first law of thermodynamics is

$$dm = TdS + \psi dq \quad (11)$$

where

$$\psi = \frac{\partial m}{\partial q} = \frac{1}{2\sqrt{S}} \quad (12)$$

is the potential associated with the tidal charge.

Although the solution (6) is static, in a classical quasi-stationary process the mass has to be either conserved or to slowly increase², in order to obey the second law of thermodynamics. This could happen by an accretion process. Similarly, the 5D geometry may evolve in a quasi-stationary way only such that the tidal charge is conserved or it decreases.

² For now, we disregard the Hawking radiation, which is negligible for astrophysical black holes.

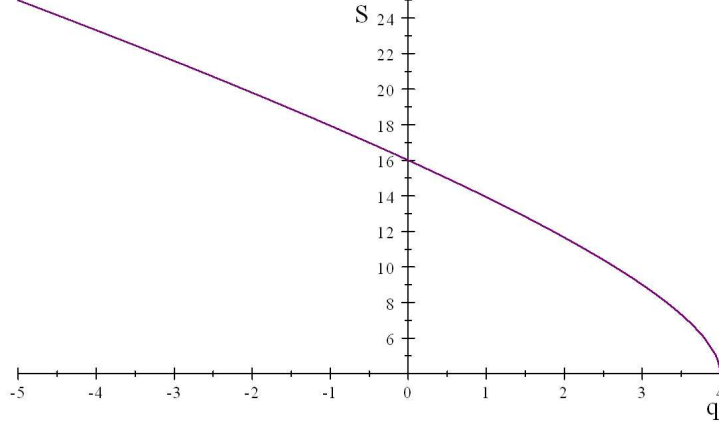


Figure 2: The qualitative behaviour of entropy vs. tidal charge. The entropy decreases with increasing q . The plot is for $m = 2$.

B. Hawking temperature and heat capacity

By the first law of thermodynamics, the Hawking temperature of the BH is given by

$$T(m, q) = \partial_S m = \frac{1}{\partial_m S} = \frac{\Theta}{2(m + \Theta)^2}. \quad (13)$$

The same value $T(m, q)$ is found by computing the temperature of the Hawking radiation if one uses the well-known formula for the surface gravity of a spherically symmetric Killing horizon (see e.g. [46]).

The temperature $T(m, q)$ increases with q for $q < 0$ up to the maximal value $T = 1/(8m)$ at $q = 0$, then decreases with increasing $q > 0$ down to $T = 0$, which is reached in the extremal limit ($q = m^2$). Thus the minimal entropy belongs to $T = 0$ and the hottest BH with a given mass is for $q = 0$, representing the Schwarzschild BH.

The heat capacity of this BH at constant q is given by

$$C_q = \frac{\partial m}{\partial T} = T \frac{\partial S}{\partial T} = T \left(\frac{\partial T}{\partial S} \right)^{-1} = T \left(\frac{\partial^2 m}{\partial S^2} \right)^{-1} = \frac{-2S(S - q)}{S - 3q}. \quad (14)$$

We can readily observe that the heat capacity diverges along $S = 3q$ or equivalently $q = 3m^2/4$. No such behaviour occurs for any $q < 0$ (for which we always have $-\infty < C_q < 0$). In (m, q) -coordinates we can express the heat capacity as

$$C_q = 2\Theta \frac{(m + \Theta)^2}{m - 2\Theta}. \quad (15)$$

Plotted against Θ , the heat capacity is shown in Fig 3.

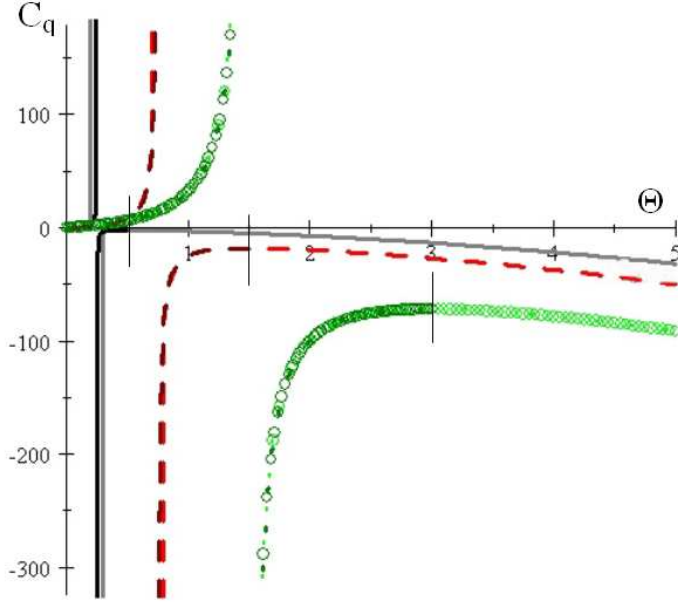


Figure 3: The heat capacity C_q as function of Θ for $m = 0.5$ (solid curve), $m = 1.5$ (dashed curve) and $m = 3$ (dotted curve). All these curves show a vanishing heat capacity in the extremal case (at $\Theta = 0$) and a divergent behaviour at $\Theta = m/2$ (equivalent to $q = 3m^2/4$ or $S = 3q$). Up to the Schwarzschild limit (at $\Theta = m$, marked with a bar on the graphs) the curves apply both for tidal-charged black holes and for Reissner-Norström black holes (with electric charge $Q = \sqrt{q}$). The region of the curves for $\Theta > m$ (thus $q < 0$) applies only for tidal-charged black holes.

The first derivative of the heat capacity at constant charge is given by

$$\frac{dC_q}{d\Theta} = \frac{2(m^2 - \Theta^2)(m + 4\Theta)}{(m - 2\Theta)^2} \quad (16)$$

become singular at $\Theta = m/2$, that is at $q = 3m^2/4$. In the domain of its negative values the heat capacity reaches a local maximum at the Schwarzschild configuration ($\Theta = m$), as can be seen from both Eq. (16) and Fig 3.

The thermodynamical interpretation of negative heat capacity is that such a BH cannot be in a stable equilibrium with an infinite heat reservoir held at $T = T_{BH}(m, q)$. For instance, a small thermal fluctuation may transfer some heat to the BH and make the BH colder, thus making heat transfer even more efficient. This is the typical behavior of Schwarzschild BHs, which are unstable with respect to emission of Hawking radiation in empty space and can be stable only in thermal contact with a finite-volume reservoir. Since the Universe may be considered as an infinite heat reservoir having the temperature of the cosmic background radiation, these considerations may be relevant to the cosmological stability of primordial or near-extremal BHs that have very low

temperature. A near-extremal BH with tidal charge $q > 3m^2/4$ has a positive heat capacity and thus can remain in a stable equilibrium with an infinite heat reservoir at $T = T_{BH}$.

Nevertheless, Schwarzschild BHs are known to be linearly stable with respect to perturbations which are nonvanishing on the bifurcation two sphere [37].

C. Poincaré stability analysis

In this subsection we address the issue of microcanonical stability of the tidal charged BH by using the so-called Poincaré method (see *e.g.* [38–40]) which has been used to decide whether critical phenomena or change of stability occurs in BH systems. The method is based on analyzing a conjugacy diagram (with a conjugacy parameter, in our case the inverse temperature, plotted against a control parameter, in our case the mass) by monitoring the change in the convexity/concavity of the curve around any occurring "turning point". According to this method there is a change of stability whenever the concavity/convexity of the curve changes at a turning point.

We plot the conjugacy diagram of the tidal charged BH for $q = 0.25$ in Fig 4. In the extremal limit, at $m = 0.5$, the curve goes to infinity. The Davies point where the heat capacity diverges [41] is at $m = 0.577$. As the curve has no turning point at all, according to the Poincaré method there is no change of stability in any point, in particular neither in the Davies point.

III. THERMODYNAMIC GEOMETRY

In this section we analyze the information geometries of the tidal charged BH.

A. The Ruppeiner metric

The geometry of the tidal charged BH depends on two parameters: m and q . From the generic definition (2) we find the corresponding Ruppeiner metric as

$$ds_R^2 = \frac{1}{\Theta^3} \left[2(m - 2\Theta)(m + \Theta)^2 dm^2 - 2(m^2 - \Theta^2)dm dq + \frac{m}{2} dq^2 \right]. \quad (17)$$

The Ruppeiner curvature scalar is

$$R = \frac{1}{2\Theta(m + \Theta)} \quad (18)$$

It is readily seen that *the curvature scalar diverges in the extremal limit* for $q > 0$, but stays regular for any $q < 0$. It is also worth to remark that at the Davies point the Ruppeiner metric becomes

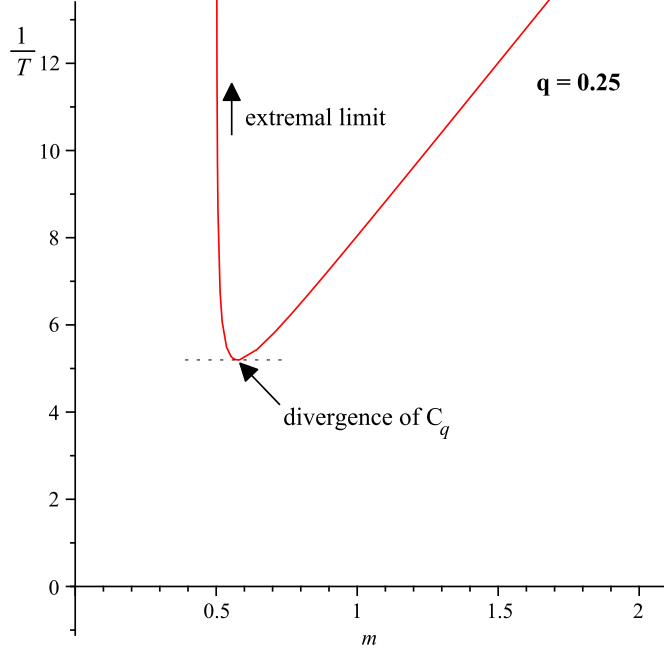


Figure 4: A conjugacy diagram (inverse temperature vs. mass) of the tidal charged BH for $q = 0.25$. The extremal limit is at $m = 0.5$ where the curve goes to infinity. There is no "turning point", so even at $m = 0.577$, the Davies point (where the heat capacity diverges), the stability holds.

degenerate (the coefficient of dm^2 vanishes). We note here that *for Reissner-Nordström BHs the situation was identical*: a singularity in the heat capacity also emerged [9] when the metric became degenerate, and was not accompanied by a phase transition.

B. The Weinhold metric

By passing to coordinates (m, Θ) in the Ruppeiner metric and using the conformal relation (4) as well as the expression for the temperature (13), we obtain the Weinhold metric explicitly as

$$ds_W^2 = T ds_R^2 = \frac{-(m + 2\Theta) dm^2 - 2\Theta dm d\Theta + m d\Theta^2}{(m + \Theta)^2}. \quad (19)$$

This can be further simplified by introducing the new coordinate r_+ replacing Θ :

$$ds_W^2 = \frac{dr_+}{r_+} \left(m \frac{dr_+}{r_+} - 2dm \right), \quad (20)$$

then passing to $(Z = \log r_+, W = \log(r_+/m^2))$ we find

$$ds_W^2 = m dZ dW, \quad (21)$$

with

$$m = \exp\left(\frac{Z - W}{2}\right). \quad (22)$$

In the coordinates $(U_+ = 2 \exp(Z/2), U_- = 2 \exp(-W/2))$ the Weinhold metric becomes *manifestly flat*, $ds_W^2 = -dU_+ dU_-$. One can also introduce Minkowskian coordinates as $U_\pm = X \pm Y$, finding $ds_W^2 = -dX^2 + dY^2$. The sequence of coordinate transformations leading to this result can be summarized as

$$\begin{aligned} X &= \sqrt{r_+} + \frac{m}{\sqrt{r_+}}, \\ Y &= \sqrt{r_+} - \frac{m}{\sqrt{r_+}}. \end{aligned} \quad (23)$$

The inverse transformation is

$$\begin{aligned} 4r_+ &= (X + Y)^2, \\ 4m &= X^2 - Y^2. \end{aligned} \quad (24)$$

C. Direct derivation of the Weinhold metric

As a further consistency check of our calculations we express from Eq. (9) the mass m of the tidal charged BH in (S, q) coordinates, obtaining

$$m = \frac{\sqrt{S}}{2} \left(1 + \frac{q}{S}\right) \quad (25)$$

This allows to calculate the Weinhold metric directly from its definition:

$$ds_W^2 = \frac{3q - S}{8S^{5/2}} dS^2 - \frac{1}{2S^{3/2}} dS dq. \quad (26)$$

It can easily be checked that the above metric is flat. When $S = 3q$ (in the Davies point, where the heat capacity diverges) the Weinhold metric is also degenerate. By performing a transformation to (m, Θ) coordinates, we recover the form (19) of the Weinhold metric.

D. The global structure of the Ruppeiner geometry

The expression of the temperature in the (X, Y) coordinates is

$$T = \frac{r_+ - m}{2r_+^2} = \frac{4Y}{(X + Y)^3}, \quad (27)$$

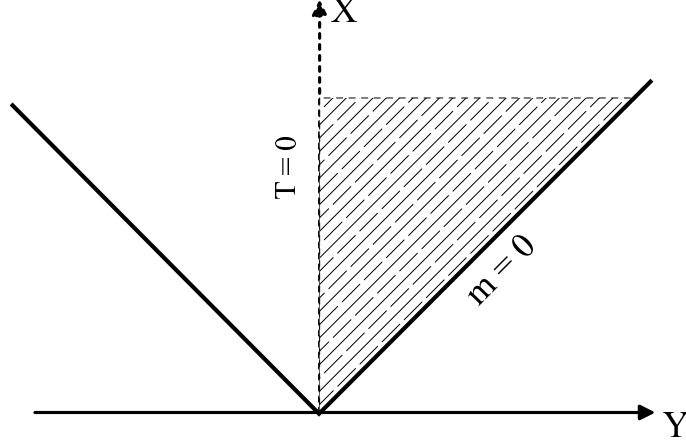


Figure 5: A state space plot of the tidal charged BH embedded in the flat Minkowskian parameter space. Note that the thermodynamic light cone (TLC) describes $m = 0$ and the wedge fills the right half of the TLC with the TLC itself excluded. The vertical axis represents the extremal limit in which $T = 0$.

which leads to the manifestly conformally flat form of the Ruppeiner metric:

$$ds_R^2 = \frac{(X+Y)^3}{4Y} (-dX^2 + dY^2) . \quad (28)$$

Note that the domain of the original Ruppeiner coordinates is

$$m \in (0, \infty), \quad q \in (-\infty, m^2) . \quad (29)$$

The corresponding ranges of the variables Θ, r_+ are $\Theta \geq 0, r_+ \geq 0$; the Minkowskian coordinates defined by (23) have the range $X > Y \geq 0$. Thus the state space is equivalent to the right half of the interior of the future light cone of a Minkowski plane, with the vertical boundary included but the light-like boundary excluded. (The light cone describes $m = 0$ states as can be seen from $4m = X^2 - Y^2$, which for $q \geq 0$ does not correspond to BH metrics.) The extremal states are located at $(X = 2\sqrt{m} > 0, Y = 0)$, i.e. on the positive half of the time-like coordinate axis (the vertical boundary). This can be also seen by writing the curvature scalar (18) of the Ruppeiner metric in the (X, Y) coordinates:

$$R = \frac{1}{2(r_+ - m)r_+} = \frac{4}{Y(X+Y)^3} . \quad (30)$$

We also remark that passing to the (X, Y) coordinates by the transformation (24) induces a degeneracy. For each pair of coordinates (m, q) , as well as for (m, Θ) or (m, r_+) , we can associate any of the combinations $(\pm X, \pm Y)$, with X, Y defined by Eq. (23). Therefore the light cone of the Minkowski plane provides a four-fold coverage of the original state space. This is similar to the introduction of the well-known Kruskal coordinates for the Schwarzschild geometry: Kruskal

coordinates cover four patches in the Kruskal-Szekeres diagram, while the original coordinates cover only one patch. See Fig. 5.

IV. COMPARISON AND PHYSICAL INTERPRETATION OF THERMODYNAMIC PROPERTIES FOR THE TIDAL CHARGED AND REISSNER-NORDSTRÖM BHs

After the generic consideration on the tidal charged BH thermodynamics made in Section II and the detailed analysis of the related information geometries in Section III, we are able to compare the tidal charged BH and the general relativistic Reissner-Nordström BH from a thermodynamic point of view.

The entropy of a Reissner-Nordström BH still obeys Eq. (9), but with $\Theta_{RN} = \sqrt{m^2 - Q^2}$. Its Ruppeiner geometry is flat, while the curvature scalar of its Weinhold geometry in (S_{RN}, Q) coordinates is [9]

$$R_W^{RN} = \frac{2S_{RN}^{3/2}}{(S_{RN} - Q^2)^2}. \quad (31)$$

We can rewrite this in the (m, Θ_{RN}) coordinates as

$$R_W^{RN} = \frac{m + \Theta_{RN}}{2\Theta_{RN}^2}. \quad (32)$$

The temperature of the Reissner-Nordström BH is [9]:

$$T_{RN} = \frac{1}{4S_{RN}^{1/2}} \left(1 - \frac{Q^2}{S_{RN}} \right). \quad (33)$$

In the (m, Θ_{RN}) coordinates it reads

$$T_{RN} = \frac{\Theta_{RN}}{2(m + \Theta_{RN})^2}, \quad (34)$$

which has the same functional form as Eq. (13).

Summarizing (a) the temperatures of the general relativistic Reissner-Nordström BH and tidal charged BH have the same functional form, and (b) both information geometries are regular for both of the BHs, with the sole exception of the extremal configurations, where the Ruppeiner metric for the tidal charged BH and the Weinhold metric for the Reissner-Nordström BH diverge. The other two information geometries are flat. The comparison of the information geometries of the two BHs is presented in Table I.

In order to see how this fits into a more generic context, we reproduce here a comparative table II of the information geometries for various BHs, given first in [42].

Table I: Ruppeiner and Weinhold information geometries for the Reissner-Nordström and tidal charged black holes. As the state space for the information geometries is two-dimensional, the respective geometries are fully characterized by the curvature scalars (second and third columns). The conformal factor relating the Weinhold and Ruppeiner geometries is the temperature of the respective black holes (fourth column).

	Weinhold	Ruppeiner	temperature
Reissner-Nordström BH	$R_W^{RN} = \frac{m+\Theta_{RN}}{2\Theta_{RN}^2}$	$R_R^{RN} = 0$	$T_{RN} = \frac{\Theta_{RN}}{2(m+\Theta_{RN})^2}$
tidal charged BH	$R_W^{tidal} = 0$	$R_R^{tidal} = \frac{1}{2\Theta(m+\Theta)}$	$T = \frac{\Theta}{2(m+\Theta)^2}$

Table II: Comparison of information geometries for various black holes.

Spacetime dimension	Black hole family	Ruppeiner	Weinhold
$d = 2$	(1+1) RN like BH (generic)	Curved	Curved
	(1+1) reduced RN BH	Flat	Curved
	(1+1) CS like BH (generic)	Curved	Flat
$d = 3$	(2+1) BTZ	Flat	Curved
	(2+1) BTZ (Chern-Simons)	Flat	Curved
	(2+1) BTZ (Log corrections)	Curved	Curved
$d = 4$	RN	Flat	Curved
	Kerr	Curved	Flat
	Kerr-Newman	Curved	Curved
	Braneworld (tidal charged)	Curved	Flat
	Dilaton	Flat	Curved
$d = 5$	Kerr	Curved	Flat
	double-spin Kerr	Curved	Curved
	RN	Flat	Curved
	Black ring	Curved	Flat
any d	Kerr	Curved	Flat
	RN	Flat	Curved

The Ruppeiner metric does not have singularities for any of these BHs, with the exception of the extremal tidal charged BH. Therefore, based on generic result that instabilities are accompanied by singularities in the Ruppeiner geometry [9], [10], [38] one would not expect phase transitions for these BHs, except perhaps the extremal tidal charged configuration. Nevertheless, extremal BHs have zero temperature, therefore this is a special case which will be addressed later.

The heat capacity diverges at $q = 3m^2/4$ for tidal charged BHs, and at $Q = 3^{1/2}m/2$ for the Reissner-Nordström BH [10]. These Davies points also show up on the (T, S) diagram represented in Fig. 6. These divergences share a similar interpretation. While such a divergence is characteristic to second order phase transitions in ordinary thermodynamics, for gravitating systems the situation is changed. In both cases mentioned above, besides diverging, the heat capacity also changes sign in the respective points. According to Sorkin a microcanonical instability would occur only if the heat capacity changes sign through zero [43], which is not the case for either of the Reissner-Nordström or tidal charged BHs. This is in full agreement with the regularity of the Ruppeiner metric in the respective points.

Katz et al. have argued [40], that instabilities do not necessarily come together with divergences of the heat capacity. Their argument was based on the Poincaré stability analysis. The Poincaré stability analyses of both the Reissner-Nordström and tidal charged BHs (the latter in this paper) have shown no instabilities at the diverging heat capacity state-space configurations. Moreover, the Poincaré stability analysis does not indicate any instability at the extremal configuration either, see Fig. 4, thus the extremal tidal charged BH does not exhibit a phase transition there. Based on the idea that the extremal limit of various black hole families might themselves be regarded as critical points [17], the Reissner-Nordström extremal point ought to represent some type of phase transition. Since the Ruppeiner metric for the Reissner-Nordström black hole is flat and a Poincaré stability analysis [40] shows no sign of instability at the extremal point, therefore we conclude that there are no phase transitions associated with it. This serves as a basis for our analysis of the tidal charged black hole in the extremal limit.

We conclude this section with comments on the negative tidal charge regime. As can be seen from Fig. 6, this range has no Davies point. This is also supported by the analysis of the free energy $F = m - TS$, plotted for both the Reissner-Nordström and tidal charged cases in Fig. 7. Whereas the respective curves end at the Davies point for any value of the electric charge, in accordance with Ref. [44] (including zero charge, the Schwarzschild case), also for any positive value of the tidal charge, the curve belonging to the negative tidal charge case continues towards infinity, signalling that not even Davies points can exist for negative tidal charge.

The main message of our analysis of this section is that *neither the Reissner-Nordström, nor the tidal charged BHs allow for phase transitions* at any of their parameter values.

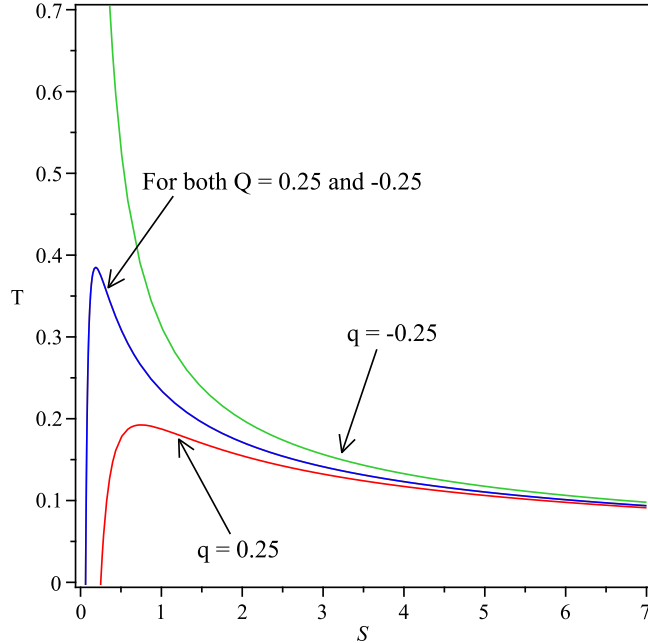


Figure 6: The (T, S) diagram for the Reissner-Nordström and tidal charged black holes. Negative tidal charged black holes are singled out in having no Davies point.

V. HAWKING LIMIT FOR TIDAL CHARGED BHs

In a seminal paper [45], Hawking has derived upper limits for the efficiency

$$\eta = 1 - \frac{m_f}{m_1 + m_2} \quad (35)$$

of mass conversion into gravitational radiation, when BHs merge. Here $m_{1,2}$ are the masses of the individual BHs and m_f is the mass of the final product. The merger of two equal mass, non-rotating BHs leads to an upper efficiency limit of $1 - 2^{-1/2} = 29.3\%$. With rotation included, the efficiency limit can increase up to 50%. The basic argument is provided by the second law of BH thermodynamics $S_f \geq S_1 + S_2$. Employing Eq. (1) for the tidal charged BHs this leads to $(m_f + \Theta_f)^2 \geq (m_1 + \Theta_1)^2 + (m_2 + \Theta_2)^2$, thus

$$m_f \geq \frac{m_1^2 \left(1 + \sqrt{1 - \frac{q_1^2}{m_1^2}}\right)^2 + m_2^2 \left(1 + \sqrt{1 - \frac{q_2^2}{m_2^2}}\right)^2 + q_f}{2 \left[m_1^2 \left(1 + \sqrt{1 - \frac{q_1^2}{m_1^2}}\right)^2 + m_2^2 \left(1 + \sqrt{1 - \frac{q_2^2}{m_2^2}}\right)^2 \right]^{1/2}}. \quad (36)$$

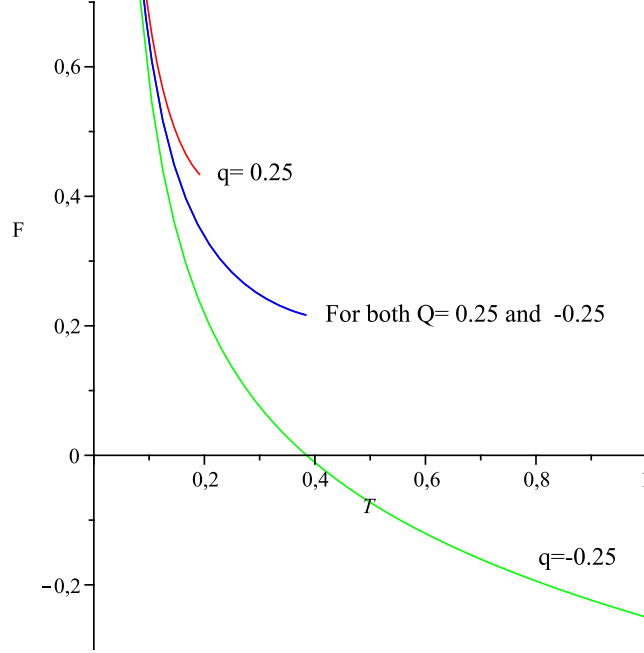


Figure 7: The free energy vs. temperature for the Reissner-Nordström and tidal charged black holes. With the exception of the negative tidal charged black hole, in all other cases the plots terminate at a finite temperature, indicating the existence of Davies points, as discussed in [44].

For identical BHs $m_2 = m_1 \equiv m$ and $q_1 = q_2 \equiv q < q_f$ (the tidal charge being an extensive parameter, as assumed throughout this paper), the efficiency limit becomes

$$\eta \leq 1 - \frac{2 + 2\sqrt{1 - \frac{q}{m^2}} - \frac{q}{2m^2} + \frac{q_f - q}{2m^2}}{2^{3/2} \left[2 + 2\sqrt{1 - \frac{q}{m^2}} - \frac{q}{m^2} \right]^{1/2}}. \quad (37)$$

This is represented on Fig. 8, as function of $q/m^2 \in (-\infty, 1]$ and $(q_f - q)/m^2 > 0$. We can derive a couple of important restrictions on the physically allowed range of the tidal charged BH parameters from this plot:

- (a) The ratio q/m^2 is bounded from below by a value $\in [-6, 0]$ depending on $(q_f - q)/m^2$.
- (b) The quantity $(q_f - q)/m^2$, a measure of the extensiveness of the tidal charge is also bounded.

Both constraints on the state space parameters come from requiring that the radiated mass cannot be more than the sum of the initial masses. To our knowledge these are the first constraints on the possible range of the tidal charge, derived in the literature.

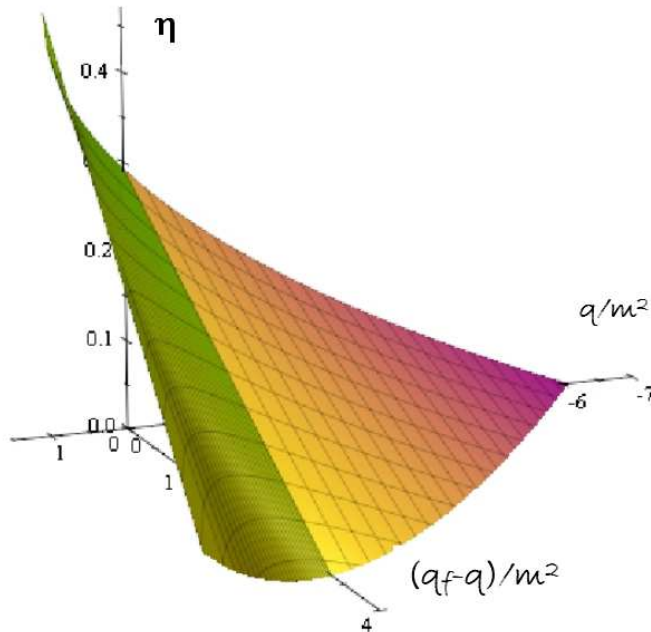


Figure 8: The efficiency limit of mass conversion into radiation for equal mass, equal tidal charged black hole collisions restricts both the values of q/m^2 and the possible value of the tidal charge of the final black hole.

VI. CONCLUDING REMARKS

We have studied the thermodynamics and thermodynamic geometries (both Ruppeiner and Weinhold) of the tidal charged brane BH. While the thermodynamic state space of the Reissner-Nordström BH is a Rindler wedge embedded in a Minkowski parameter space, the state space of the tidal charged BH is the right half of the interior of the future light cone of the Minkowski plane, with the vertical boundary included but the light-like boundary excluded. The light cone of the Minkowski plane provides a four-fold coverage of this state space, similarly to the four-fold covering of the curvature coordinates for a Schwarzschild BH by Kruskal coordinates. The geodesics of the information geometries characterize the time for *quasistatic relaxation* and *minimum dissipation*, respectively.

Whilst from the point of view of gravitational curvature the $q > 0$ case is the Reissner-Nordström geometry with electric charge $Q = \sqrt{q}$, a negative tidal charge has no correspondence in general relativity. Along the well-known property that such a negative tidal charge strengthens the gravitational field of the BH and as such contributes to the localization of gravity on the brane, our analysis has explicitly shown that $q < 0$ is also *thermodynamically preferred*, as it comes with a higher entropy.

For $q > 0$ we have found both similarities and differences as compared to the Reissner-Nordström BH. The Ruppeiner geometry having a positive Ricci curvature, as opposed to the flat Ruppeiner metric for the Reissner-Nordström BH [9], indicates that *the underlying statistical models for the two BHs could be different*.

Despite the heat capacity of the tidal charged BH diverging on a set of measure zero of the parameter space (at $q = 3m^2/4$, the Davies point), both a Poincaré stability analysis and the regularity of the Ruppeiner metric shows no indication of phase transition at that point, similarly as for the Reissner-Nordström BH and the Kerr BH [38], where (despite the change of sign of the heat capacity through infinite values at the Davies point) the BHs remains stable. Similarly for some other BHs, the induced Ruppeiner geometry of the tidal charged BH is singular in the extremal limit, but Poincaré stability analysis once again disrules the possibility of phase transition there. Therefore we have shown that *the tidal charged BH is stable for the full parameter range*.

Starting from the Hawking limit for the efficiency of gravitational radiation in a BH merger process, we have derived here for the first time *constraints on the tidal charge range*.

VII. ACKNOWLEDGMENTS

LG wishes to acknowledge discussions with Shinji Mukohyama on the relation of the entropies of higher dimensional black objects and their lower dimensional sections. He was succesively supported by the Hungarian Scientific Research Fund (OTKA) grant no. 69036, a London South Bank University Research Opportunities Fund Award, the Polnyi and Sun Programs of the Hungarian National Office for Research and Technology (NKTH), by Collegium Budapest, finally by COST Action MP0905 "Black Holes in a Violent Universe". NP would like to thank Roberto Emparan for insightful discussions and useful comments, and also wishes to acknowledge the hospitality of Departament de Física Fonamental at Universitat de Barcelona during his research visit. He was supported by Doktorandtjnst of Stockholm University during the early stage of this work and is grateful for scholarships from Helge Ax:son Johnsons stiftelse and K & A Wallenbergs stiftelse. NP would also like to acknowledge the kind hospitality of the Department of Theoretical Physics and the Department of Experimental Physics at the University of Szeged, Hungary during his recent visit funded by the Royal Swedish Academy of Sciences (KVA).

Appendix A: The general relation between the Ruppeiner and Weinhold metrics

In this Appendix we present a concise derivation of the generic statement that the Ruppeiner and Weinhold metrics (2) and (3) are conformally related, with the temperature (5) as the conformal factor.

Let us consider a scalar function³ $m(x)$ of the variables $x \equiv \{x^a \mid a = \overline{1, n+1}, n \in N\}$. We will also consider another coordinate system $y \equiv \{y^c \mid c = \overline{1, n+1}, n \in N\}$ in the same configuration space. A series expansion of $\delta m \equiv m(x + \delta x) - m(x)$ about an arbitrary point gives

$$\delta m(x) = \frac{\partial m}{\partial x^a} \delta x^a + \frac{1}{2} \frac{\partial^2 m}{\partial x^a \partial x^b} \delta x^a \delta x^b + \mathcal{O}(\delta x)^3, \quad (\text{A1})$$

$$\delta m(y) = \frac{\partial m}{\partial y^c} \delta y^c + \frac{1}{2} \frac{\partial^2 m}{\partial y^c \partial y^d} \delta y^c \delta y^d + \mathcal{O}(\delta y)^3. \quad (\text{A2})$$

It is understood that all derivatives are evaluated at the same point x_0 , and that y_0 and δy_0 represent x_0 and δx_0 expressed in the coordinates $\{y^c\}$. In particular, we have a similar expansion

$$\delta x^a(y) = \frac{\partial x^a}{\partial y^c} \delta y^c + \frac{1}{2} \frac{\partial^2 x^a}{\partial y^c \partial y^d} \delta y^c \delta y^d + \mathcal{O}(\delta y)^3. \quad (\text{A3})$$

Let us now derive a relationship between $\partial^2 m / \partial x^a \partial x^b$ and $\partial^2 m / \partial y^c \partial y^d$. By inserting Eq. (A3) into Eq. (A1), we obtain a second expression for δm as a function of the coordinates y ; that expression should coincide with Eq. (A2) order by order. By identifying the first-order and second-order contributions with the respective quantities of Eq. (A2) we obtain:

$$\frac{\partial m(y)}{\partial y^c} = \frac{\partial m(x)}{\partial x^a} \frac{\partial x^a(y)}{\partial y^c}, \quad (\text{A4})$$

$$\frac{\partial^2 m(y)}{\partial y^c \partial y^d} = \frac{\partial^2 m(x)}{\partial x^a \partial x^b} \frac{\partial x^a(y)}{\partial y^c} \frac{\partial x^b(y)}{\partial y^d} + \frac{\partial m(x)}{\partial x^a} \frac{\partial^2 x^a(y)}{\partial y^c \partial y^d}. \quad (\text{A5})$$

While Eq. (A4) is simply the chain rule, Eq. (A5) is the identity that will eventually yield the desired result.

In order to achieve this, we specify the coordinates as follows,

$$x = \{q^1, \dots, q^n, S\}, \quad (\text{A6})$$

$$y = \{q^1, \dots, q^n, m\}. \quad (\text{A7})$$

In other words, the coordinates y^i are the same as x^i except for the last coordinate y^{n+1} , which is chosen as the function $m(x)$ itself. It then follows that

$$\frac{\partial m(y)}{\partial y^i} = \delta_i^{n+1}, \quad (\text{A8})$$

³ The function m is generic at this stage, but will be identified with the mass at the end of the Appendix.

thus the left hand side of Eq. (A5) identically vanishes. It is also straightforward to see that

$$\frac{\partial^2 x^a(y)}{\partial y^c \partial y^d} = \frac{\partial}{\partial y^d} \left[\delta_i^a \delta_c^i + \delta_{n+1}^a \frac{\partial S(y)}{\partial y^c} \right] = \delta_{n+1}^a \frac{\partial^2 S(y)}{\partial y^c \partial y^d}. \quad (\text{A9})$$

Thus Eq. (A5) is reduced to the identity

$$\frac{\partial^2 m(x)}{\partial x^a \partial x^b} \frac{\partial x^a(y)}{\partial y^c} \frac{\partial x^b(y)}{\partial y^d} = - \frac{\partial m(x)}{\partial S} \frac{\partial^2 S(y)}{\partial y^c \partial y^d}. \quad (\text{A10})$$

By recalling the definitions (2), (3) and (5) of the Ruppeiner metric, Weinhold metric and temperature, respectively, by having in mind that the set of coordinates x and y are given by Eqs. (A6)-(A7), we have recovered the desired relation

$$g_{ab}^W(x) \frac{\partial x^a}{\partial y^c} \frac{\partial x^b}{\partial y^d} = T g_{cd}^R(y), \quad (\text{A11})$$

where the left hand side represents the Weinhold metric transformed to the y coordinates.

Appendix B: The geodesics of the thermodynamic metrics

The interpretation of the thermodynamic metrics is the following. A Weinhold geodesic (the path of least Weinhold length) in the parameter space corresponds to a quasistatic process that, in a well-defined sense, *optimizes the “thermodynamical time”*, which roughly means the time necessary for *quasistatic relaxation* during the process [47]. Since in the present case the Weinhold metric is flat, its geodesics are straight lines both in the Minkowskian coordinates (X, Y) and in the null coordinates $U_{\pm} = X \pm Y$:

$$U_+ = \alpha U_- + \beta, \quad (\text{B1})$$

with α, β constants.

On the other hand, the “length” of a process computed in the Ruppeiner metric describes the *minimum dissipation* (increase of entropy) that is unavoidable in a quasistatic process [48]. The geodesic equations for the Ruppeiner metric are the simplest when written in the conformally Minkowskian null coordinates U_{\pm} :

$$\begin{aligned} \frac{d^2 U_+}{d\lambda^2} + \frac{2U_+ - 3U_-}{U_+ (U_+ - U_-)} \left(\frac{dU_+}{d\lambda} \right)^2 &= 0, \\ \frac{d^2 U_-}{d\lambda^2} + \frac{1}{U_+ - U_-} \left(\frac{dU_-}{d\lambda} \right)^2 &= 0, \end{aligned} \quad (\text{B2})$$

with λ an affine parameter.

[1] J. M. Bardeen, B. Carter and S.W. Hawking, Commun. Math. Phys. **31** 161 (1973).

- [2] A. Strominger and C. Vafa, Phys. Lett. B **379**, 99 (1996) [arXiv:hep-th/9601029].
- [3] G. Ruppeiner, Phys. Rev. A **20**, 1608 (1979).
- [4] G. Ruppeiner, Rev. Mod. Phys. **67**, 605 (1995).
- [5] B. Mirza and H. Mohammadzadeh, Phys. Rev. E **80**, 011132 (2009) [arXiv:0808.0241 [cond-mat]].
- [6] D. A. Johnston, W. Janke and R. Kenna, Acta Phys. Polon. B **34**, 4923 (2003) [arXiv:cond-mat/0308316].
- [7] J. E. man and N. Pidokrajt, Phys. Rev. D **73**, 024017 (2006) [arXiv:hep-th/0510139].
- [8] R. Emparan and R. C. Myers, JHEP **0309**, 025 (2003) [arXiv:hep-th/0308056].
- [9] J. E. man, I. Bengtsson and N. Pidokrajt, Gen. Rel. Grav. **35**, 1733 (2003) [arXiv:gr-qc/0304015].
- [10] J. E. man, I. Bengtsson and N. Pidokrajt, Gen. Rel. Grav. **38**, 1305 (2006) [arXiv:gr-qc/0601119].
- [11] J. E. man, *et al.* J. Phys. Conf. Ser. **66**, 012007 (2007) [arXiv:gr-qc/0611119].
- [12] T. Sarkar, G. Sengupta and B. Nath Tiwari, JHEP **0611**, 015 (2006) [arXiv:hep-th/0606084].
- [13] B. Mirza and M. Zamani-Nasab, JHEP **0706**, 059 (2007) [arXiv:0706.3450 [hep-th]].
- [14] H. Quevedo, Gen. Rel. Grav. **40**, 971 (2008) [arXiv:0704.3102 [gr-qc]].
- [15] G. Ruppeiner, Phys. Rev. D **78**, 024016 (2008) [arXiv:0802.1326 [gr-qc]].
- [16] J. L. Alvarez, H. Quevedo and A. Sanchez, Phys. Rev. D **77**, 084004 (2008) [arXiv:0801.2279 [gr-qc]].
- [17] J. Louko and S. N. Winters-Hilt, Phys. Rev. D **54**, 2647 (1996) [arXiv:gr-qc/9602003]. A. Chamblin, R. Emparan, C. V. Johnson and R. C. Myers, Phys. Rev. D **60**, 104026 (1999) [arXiv:hep-th/9904197]. Y. S. Myung, Y. W. Kim and Y. J. Park, Phys. Lett. B **663**, 342 (2008) [arXiv:0802.2152 [hep-th]].
- [18] A. J. M. Medved, Mod. Phys. Lett. A **23**, 2149 (2008) [arXiv:0801.3497 [gr-qc]].
- [19] J. Shen, R.-G. Cai, B. Wang and R.-K. Su, Int. J. Mod. Phys. A **22**, 11 (2007) [arXiv:gr-qc/0512035].
- [20] F. Weinhold, J. Chem. Phys. **63**, 2479 (1975).
- [21] P. Salamon, J. Nulton and E. Ihrig, J. Chem. Phys. **80**, 436 (1984).
- [22] T. Shiromizu, K.I. Maeda and M. Sasaki, Phys. Rev. D **62**, 024012 (2000) [arXiv:gr-qc/9910076].
- [23] L. Á. Gergely, Phys. Rev. D **68**, 124011 (2003) [arXiv:gr-qc/0308072].
- [24] L. Á. Gergely, Phys. Rev. D **78**, 084006 (2008) [arXiv:0806.3857 [gr-qc]].
- [25] N. Dadhich, R. Maartens, P. Papadopoulos and V. Rezanian, Phys. Lett. B **487**, 1 (2000) [arXiv:hep-th/0003061].
- [26] Y. S. Myung, Y. W. Kim and Y. J. Park, Phys. Rev. D **78**, 084002 (2008) [arXiv:0805.0187 [gr-qc]].
- [27] R. Casadio, O. Micu., Phys. Rev. D **81**, 104024 (2010) [arXiv:1002.1219]
- [28] R. Casadio, S. Fabi, B. Harms, O. Micu, [arXiv: 0911.1884]
- [29] C. Germani and R. Maartens, Phys. Rev. D **64**, 124010 (2001) [arXiv:hep-th/0107011].
- [30] L. Á. Gergely and B. Darázs, Publ. Astron. Dept. Etsv Univ. PADEU **17**, 213 (2006) [arXiv:astro-ph/0602427].
- [31] L. Á. Gergely, Z. Keresztes and M. Dwornik, Class. Quantum Grav. **26**, 145002 (2009) [arXiv:0903.1558 [gr-qc]].
- [32] Z. Horváth, L. Á. Gergely and D. Hobill, Class. Quantum Grav. **27**, 235006 (2010) [arXiv: 1005.2286]

[gr-qc].

- [33] C. G. Boehmer, T. Harko and F. S. N. Lobo, *Class. Quant. Grav.* **25**, 045015 (2008) [arXiv:0801.1375].
- [34] C. S. J. Pun, Z. Kovacs and T. Harko, *Phys. Rev. D* **78**, 084015 (2008) [arXiv:0809.1284].
- [35] R. Emparan, G. T. Horowitz and R. C. Myers, *JHEP* 0001 021 (2000) [arXiv:hep-th/9912135].
- [36] A. Chamblin, R. Emparan, C. J. Johnson, and R. C. Myers, *Phys. Rev. D* **60**, 064018 (1999).
- [37] B. S. Kay and R. M. Wald, *Class. Quantum Grav.* **4**, 893 (1987).
- [38] G. Arcioni and E. Lozano-Tellechea, *Phys. Rev. D* **72**, 104021 (2005) [arXiv:hep-th/0412118].
- [39] O. Kaburaki, I. Okamoto and J. Katz, *Phys. Rev.* **D47** (1993) 2234.
- [40] J. Katz, I. Okamoto and O. Kaburaki, *Class. Quant. Grav.* **10**, 1323 (1993).
- [41] P. C. W. Davies, *Proc. Roy. Soc. Lond. A* **353**, 499-521 (1977).
- [42] N. Pidokrajt, Ph. D. Thesis, Stockholm University (2009).
- [43] R. Sorkin, *Astrophys. J.* **257**, 847 (1982).
- [44] H. La, [arXiv:1010.3626] (2010).
- [45] S. Hawking, *Phys. Rev. Lett.* **26**, 1344 (1971).
- [46] T. Padmanabhan, *Phys. Rept.* **406**, 49 (2005) [arXiv:gr-qc/0311036].
- [47] L. Diósi, K. Kulacsy, B. Lukács and A. Rácz, *J. Chem. Phys.* **105**, 11220 (1996).
- [48] J. Nulton, P. Salamon, B. Andresen and Qi Anmin, *J. Chem. Phys.* **83**, 334 (1985).